ENCIT 2018

ABCM Associação Brasileira de Engenharia e Ciências Mecânicas

17th Brazilian Congress of Thermal Sciences and Engineering
November 25th-28th, 2018, Águas de Lindóia, SP, Brazil

EXPERIMENTAL STUDY OF OXY-FUEL COMBUSTION IN A COFLOW BURNER

Vitor Augusto Andreghetto Bortolin
Bernardo Luiz Harry Diniz Lemos
Guenther Carlos Krieger Filho
Universidade de São Paulo, Escola Politécnica, Engenharia Mecânica – Av. Professor Mello Moraes 2231, Cidade Universitária. São Paulo/SP. Brazil
vitorbortolin0@gmail.com
bernardolemos@usp.br
guenther@usp.br

Abstract. *Carbon Capture and Storage (CCS) technology aims to extend the lifespan of fossil fuel in the energy matrix and allow a smooth transition to renewable energy. However, the high cost prevents its used. To overcome this difficulty, the oxy-fuel concept has been proposed, allowing a reduction in the costs. Though it presents its owns challenges. The combustion in carbon dioxide rich environments reduces the reaction rates, flame stability and combustion efficiency. To improve oxy-fuel combustion, this work aims to evaluate experimentally a methane and liquefied petroleum gas (LPG) diffusion flame in different oxidizer compositions. A standard burner denoted hereafter as "Yale burner" is employed. The cold flow velocity field is evaluated using a constant temperature anemometer (CTA), whereas chemiluminescence is used to analyze the combustion. Observing the light emission of CH radical. The results shown that the burner coflow design provides a homogeneous flow. While in the chemiluminescence the oxy-fuel flame showed a different behavior than it air counterpart. It was smaller and could only be kept stable with higher oxygen concentration than the one in air. Also present an inferior proportional emission in the CH* light range.*

Keywords: *oxy-fuel, chemiluminescence , hot wire anemometry, Carbon Capture and Storage*

1. INTRODUCTION

The recent environmental concern leads to increase research in the Carbon Capture and Storage(CCS) technology, which enables the use of fossil fuels with great reduction in emissions. However, the costs associated with this technology are still prohibitive. Therefore, research efforts focus on the reduction of the capital and energy cost associated with this technology. In the review presented by Leung *et al.* (2014), the expenditure from the capture process(separation of the CO_2 from the exhaust stream) were estimated to be between 70 to 80% of the total cost of a full CCS system. Thus most alternatives aim at this particular phase. A proposal to reduce these costs is the oxy-fuel combustion in which the common oxidizer, air, is exchanged for a mixture of oxygen and carbon dioxide resulting in an exhaust stream of only water vapor and carbon dioxide that can be easily separated. The advantages of this technology are the high reduction in capture cost and minimization of the store volume. Notwithstanding, significantly changes in the combustion process have been shown (Scheffknecht *et al.*, 2011; Sundkvist *et al.*, 2014; Chen *et al.*, 2012) to affect the flame temperature, flame stability, soot production, corrosion, and heat transfer. Therefore, the investigation of the phenomena in this particular combustion is necessary to improve burner designs.

Most of the development in the oxy-fuel combustion had been carried by coal research. Wall *et al.* (2011) considered this technology to be in a semi-commercial state. However, recent data indicates that natural gas will became the main energy source in the next years (Birol, 2017). To exemplify the global share of natural gas on 2017, the total primary energy production from natural gas evened that from coal. Therefore, in a long term, CCS strategies for gas power plants will be necessary.

Sundkvist *et al.* (2014) analyses different cycle possibilities for an oxy-fuel gas power plant and highlights the main difficulties. To minimize the oxygen consumption, an expensive input, the combustion chamber need to work in almost stoichiometric. This may result in improper fuel burn, increased CO production, flame instabilities. The author simulation estimates the laminar flame speed of a stoichiometric methane in oxy-fuel to be around 10 cm/s, with an oxygen content of 21% (same as air). This is just one fourth of methane-

air laminar flame velocity, this entails difficulties in stabilizes the flame and consequently reduction in the combustion efficiency. This simulations contribute to the understanding that the reaction rates are reduced in the oxy-fuel. To achieve, the same reaction rates of air Sundkvist *et al.* (2014) an oxygen concentration of 38% was needed. However, the author remarks that this increases the flame temperature above what is currently possible for turbines. To overcome these difficulties, most proposal designs for oxy-fuel combustion chamber has two distinct oxidizer streams, each one with different oxygen concentration. In principle, this could mitigate most difficulties and even achieve great performance than regular chambers. Meanwhile, this extra design variable increase the complexity and is beyond conventional combustion modeling.

De Persis *et al.* (2013) evaluated experimentally the laminar flame speed with different mixtures of oxygen, nitrogen and carbon dioxide as oxidizer. The author compare the experimental results with a simulation done with GRI3.0 and found a good agreement validating the reaction model for the oxy-fuel environment. Besides that, a fast decrease in flame speed with the increase of CO_2 concentration was observed. To better understand this change Giménez-López *et al.* (2015) measured the oxidation of methane with a gas chromatography. The authors conclusion corroborates with the assumption that the current chemical model for methane combustion is appropriated for the oxy-fuel combustion. In this case, others chemical branches have a greater impact in the overall reaction. The large amount of CO_2 change the equilibrium in reaction 1, this consumes H radicals decreasing the velocity in all the reaction here this radical participates.

$$CO + OH \leftrightarrow CO_2 + H \tag{1}$$

In combustion chamber the decrease in reaction rates can lead to local extinction, instabilities, pollutant production and a reduction in the combustion efficient.

2. OBJECTIVES

This experimental work aim to study the behavior a laminar diffusion flame in an oxy-fuel environment. The acquire data includes the punctual characterization of the turbulent field in the burner and qualitative and quantitative evaluation of the total light emission and CH radical emission during the oxy-fuel combustion.

3. BURNER

The selected burner has been manufactured based on Smooke *et al.* (1999) for the study of soot formation in laminar diffusion flames. Figures 1a and 1b, shows the burner and a section view of the project. In this configuration, fuel is injected in the middle of a cold oxidant stream. The fuel inlet is a stainless steel tube with an outer diameter of 3/16"(4.76 mm). The Coflow gas enters the base of the burner through four entries with 1/8" NPT connections. The main body of the burner consists of a cylinder with an outer diameter of 89 mm and with a length of 82 mm. There is a center hole with a diameter of 76 mm from the base to the height of 32 mm, preposterously there is a contraction that reduces the hole diameter to 73 mm by a length of 45 mm, and in the last 5 mm the diameter returns to 76 mm. To homogenize the flow, two honeycombs of Hasteloy-X ®, with a cell size of 0.79 mm (1/32 "), are positioned in the Coflow, where one was positioned at the base and another at the top of the burner. They are fixed only by engagement without any type of seal. Between them the space is filled with glass beads with an average diameter of 3 mm. Disregarding the fuel injector the burner was manufactured from aluminum. Only a minor change was made in relation to the original design, in the lower lid of the burner, where was added a conical structure to aid positioning the tube and hold the honeycomb. In addition, peripheral parts for fixing the burner on the experimental bench were manufactured of aluminum.

There is an extensive literature review of this burner, covering soot formation, transient flame, sound and combustion interaction and optical laser measurement (Bennett *et al.*, 2001; Smooke *et al.*, 2005; Dworkin *et al.*, 2007). Numerical simulations are also available for this equipment operating with air/methane flames and air/ethylene flames.

4. METHODOLOGY

Two techniques are chosen to be applied in this burner: Constant Temperature Anemometer (CTA) and chemiluminescence. The first allows to characterize the velocity and turbulent field using a probe. Limitations of this approach are two: measurements are punctual and the probe is invasive. Nevertheless, the flux conditioners in the coflow stream makes extremely difficulty to use non-invasive techniques, such as Particle Image Velocimetry (PIV). In this case, most PIV tracers will be trapped in the conditioners. Dworkin *et al.* (2007) was able to do PIV measurements, but the tracers were inject only thought the fuel entry. This lead to an incomplete characterization of the fields in the coflow region.

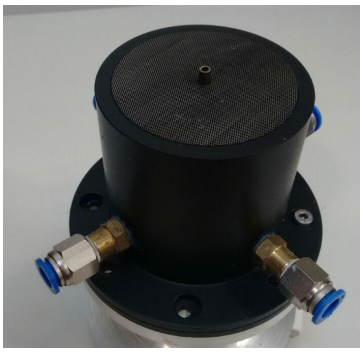

(a) Burner based on Smooke *et al.* (1999)

(b) Cross-sectional view of the project

Figure 1: The selected Burner

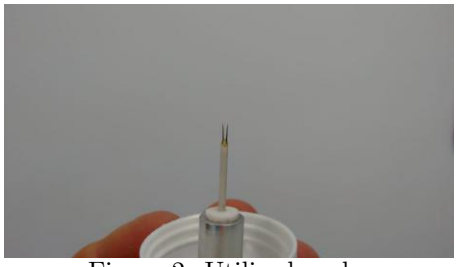

Figure 2: Utilized probe

The procedure to the CTA begins with the calibration of the probe. For all tests, a probe type 55P11 was used to measure the velocity magnitude (figure 2). The calibration interval was from 0.2 to 2 m/s and was evaluated with 18 points in an automatic calibrator. Besides, a thermocouple monitored the room temperature during the experiments to correct the measured voltage and keep the error below 2%. This small deviation is not visible in any of the velocity graphs due to the scale. The anemometer was fixed to a manual traverse that allows a displacement of 1 mm with an accuracy of 0.2 mm. A machined aluminum bracket places the traverse in the same height as the burner. In image 3b, an empty anemometer support is show right at the center of the burner in the manual centering procedure. Then the probe was installed and the measurements were performed sweeping the radius in steps of one millimeter. All the runs were done with an acquisition rate of 4 kHz acquiring 20 thousands points per measured radius.

(a) Manual traverse

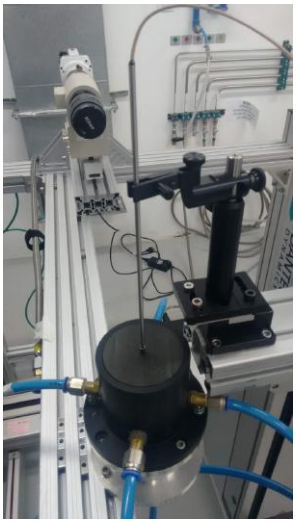

(b) Support in the center of the burner

Figure 3: CTA experimental apparatus

The chemiluminescence is the light emission by chemical species when they are excited by some chemical reaction. This effect occurs in the reaction zone, where radicals are formed in the excited configuration. In combustion, two of the main formed radicals are $OH*$ and $CH*$. The $OH*$ radical has an emission in the

band around 307 nm while the $CH*$ emission is range around 430 nm (Guiberti *et al.*, 2017). This excited radicals have a very short mean-life, therefore almost only exist in the reaction zone. The equivalence ratio in laminar premixed and non-premixed methane/air flames was numerical evaluated with the ratio of emissions light of $OH*/CH*$ by Panoutsos *et al.* (2009). This relation has a strong correlation with the equivalence ratio (ϕ) and can be used as a highlighter of the reaction zone. This occurs because the excited $OH*$ exist in the stoichiometric to lean position, while the excited $CH*$ exist in the stoichiometric to rich region. Therefore, the emission overlap only occurs in the stoichiometric. Hardalupas and Orain (2004) also estimates the heat release ratio with this relation. However, to have an accurate numerical value the broadband emission from carbon dioxide and soot need to be treated. Despite that, this ratio is an important spacial marker of the reaction zone.

To acquire the chemiluminescence emission, a set of band-pass optical filters was used. In this experiments the CH* was studied, so an optical filter with more than 90% transmission in the band 390nm to 440 nm and OD5 for the other wavelengths was selected. Besides that, two others band-pass filters were use to evaluated the background light emission which populates the entire spectrum, one with an band in the 4450-490 nm and the other in 522-542nm. Throughout the text the filter will be referred from the center of the band: 414 nm, 469 nm and 532 nm. Due to the high sensibility of the camera sensor to wavelengths in the region 380-1000 nm no image intensifier was need to acquire the signal from the CH* (figure 4). A Phantom Miro LAB 311 camera was used to acquire image in 1280 by 800 pixels with an rate of 1 kHz. In each run four thousand images were acquired. However, as the flame is in stationary regime only the mean of the was used for the analysis. In this case, the advantage in using the mean image instead of the instantaneous is the reduction of noise.

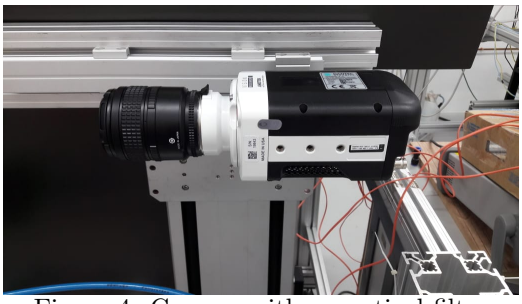

Figure 4: Camera with an optical filter

The captured image is a projection of the three-dimensional combustion region, because the light emission by the flame is a three dimensional process . It is possible to reconstruct a plane visualization from projected image using the tomographic reconstruction theory and the Radon transform (Worth and Dawson, 2012). Thought this method demand multiple images around the event taken simultaneously, and in this case it would require several cameras observing synchronously the flame. In asymmetrical objects, the Radon transform can be simplified in the Abel transform that uses only one image to reconstruct the three-dimensional structure. Smith *et al.* (2002) and De Leo *et al.* (2007) uses this approach in axisymmetrical laminar flames to quantify the light emission in the reaction region and calculate geometric parameters of the flame.

Table 1: Rotameter flow meters

Flow Meter	Operational Range(L/min)	Precision (L/min)
1	10-100	5
2	5-50	2.5
3	0.1-1	0.05

To regulate and control the gas flow, manual rotameter flow meters were used(figure 5).The operational parameters are summarized in the table 1. Two were used for the air test, number three for the fuel and number one for the coflow, and three were used for the oxy-fuel test, number three for the fuel and number one and two for the coflow. The scale used is liters per minute, all calibrated for air with an error of half of the minimum division.

A quartz cylinder with 75 mm in diameter was fixed over the burner to isolate the oxy-fuel flame from the atmosphere. The junction of this window with the burner was sealed with plastic hot glue. After the seal all the setup was tested for eventual leaks. With all leaks seal the oxy-fuel tests were performed.

Figure 5: Flow controllers

5. ANEMOMETRY RESULTS

The constant temperature anemometry has done with air injected through the fuel injector and the coflow. Table 2 shows the nominal volumetric air flow rate used during the experiments, this were the values displayed in the flow meters. The objective of this experiment is to characterize and verify the homogeneity of the air flow in the coflow region. In the first tests, the space between the two honeycombs was complete filled with glass beads. It was conjectured that this would improve the homogeneity of the flow, minimizing the effect of the inlet. However, the data show a high velocity heterogeneity with some areas reaching the inferior limit of the sensor calibration and others around 0.8 m/s. The cause of this inhomogeneous field was the interference of the glass beads with the superior honeycomb. The air fallow preferential paths through the balls and the proximity with the honeycombs keep this patterns from dissipate. After reducing the volume of glass balls to approximately half of the initial value the velocity became more evenly distributed across the coflow.

Table 2: Air Flow for anemometry

Coflow flow rate	$100L/min$
Fuel flow rate	$0.3L/min$

In figure 6, the speed profiles of the two test are shown. The average velocity for the coflow estimated by the volumetric flow is $0.419m/s$ with uncertainty of $0.05m/s$ from the regulator, the mean coflow velocity in the second experiment was $0.408m/s$ inside the margin of error. The fluctuations still observed in the half filled coflow case were due to the constructive characteristics of the burner. At the radial distance 2-4mm the edge of the fuel injection tube creates a low velocity recirculation zone. After, the junction of the honeycomb and the central duct leaks. Besides that the pipe creates a low resistance way in the glass balls layer. The combined effect of the leakage and less resistance path increase the velocity in the 4-8mm region. Finally, in the end of the coflow a similar increase is also observed. These small variations shouldn't disturb the central diffusion flame and may guarantee a stable boundary condition.

Then standard deviation of the velocity was calculated for every measured point and divided by the mean velocity to obtain the the turbulent intensity plotted in graph 7. The probe precision is limited to 2% this results in a ground for the variance, thus turbulence intensity close to 2% may be considered as noise not physical turbulence. In the middle of the fuel jet a small intensity, below 3%, points to a laminar jet. While in the nearby region, the slow velocity ahead of the corner of the fuel injector and the shear between different flow speeds generates a higher turbulence amid the rays of 4 and 12 mm. Next, the turbulent intensity becomes stable among 4%-5% through the rest of the coflow.

6. CHEMILUMINESCENCE RESULTS

The reactive flow experiments were divided in two main runs: the first the flame is in coflow of air and in the second in a coflow of oxygen and carbon dioxide. The air setup is used as a reference for comparison with the oxy-fuel test. Table 3 summarizes the parameters utilized across all test. The coflow volumetric flow rate was kept constant to avoid differences due to velocity changes in the boundaries. Besides that, its composition

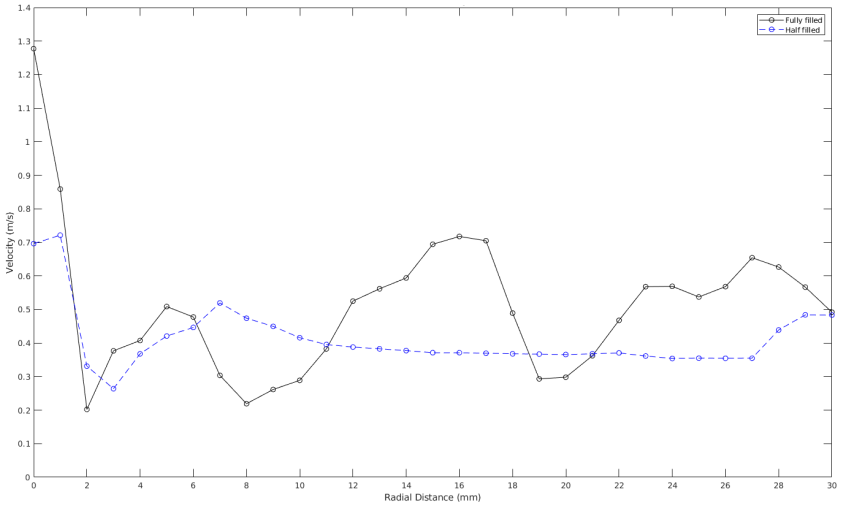

Figure 6: Velocity magnitude in the Burner

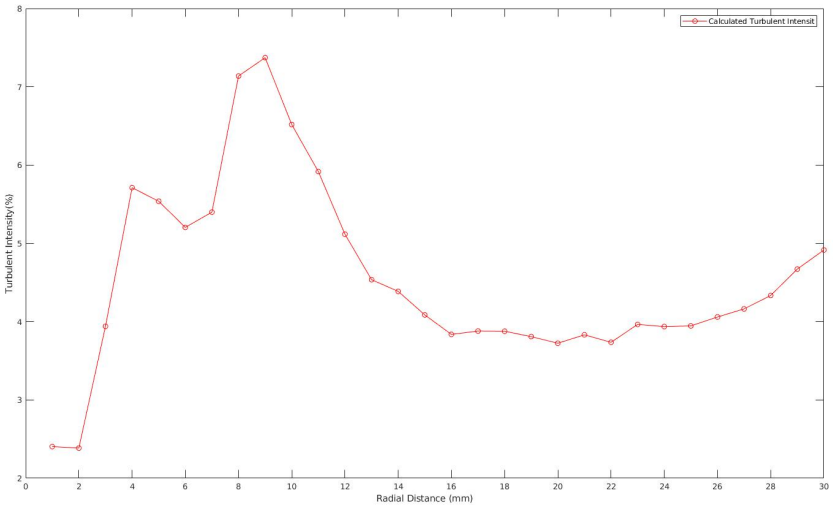

Figure 7: Turbulent Intensity in the Burner

varied in the values exposed in table 3. Finally, the fuel output was choose nearby the flow rate tested in the anemometer, and the difference between LPG and methane aims to keep approximately the same power in both flames.

Table 3: Experimental Parameters

Oxygen Content in Coflow	50%-40%-35%-30%
Carbon Dioxide Content in Coflow	50%-60%-65%-70%
LPG nominal flow rate	0.2 L/min
Methane nominal flow	0.35 L/min
LPG corrected flow rate	0.15 L/min
Methane corrected flow rate	0.47 L/min
Coflow flow rate	100 L/min

Before the actual measurements, the camera was focus on the interest region. A checkerboard target was positioned in the center of the fuel injector to assist the process. This target has a double purpose was also used to establish a correlation between pixel and spacial distance. For the reference experiments with an air, coflow image 8a of the target was used for calibration. Using the automatic routine present in MATLAB, the distance

in pixels between corners was found. This gave a correlation across the pattern of 43 pixels for every 5 mm. So every pixel represents a spacial length of 0.116 mm. For the oxy-fuel experiment, two images were taken(figures 8b and 8c) to study the image distortion that the cylindrical quartz window could cause. Fortunately, no detectable difference among the two images has found in the interest region and the pixel distance relation remain the same(0.116mm/pixel).

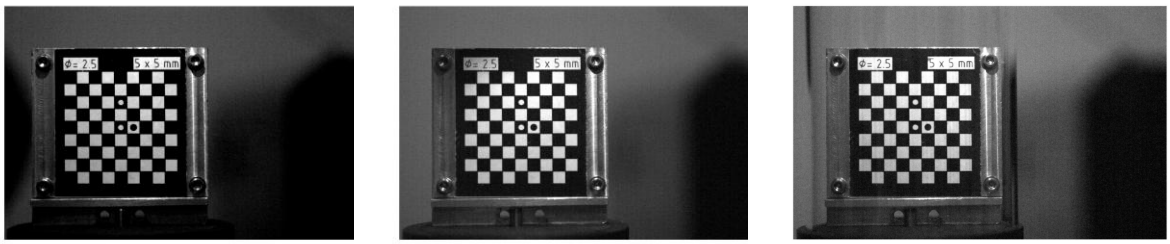

(a) Test with air (b) Test Oxy-fuel (c) Test Oxy-fuel with window

Figure 8: Pictures of the Calibrator

After the calibration, the experiments with air coflow were done. Each flame was evaluated with four mean images, one with no optical filter and the other three with the filters: 532 nm, 469 nm and 414 nm. The signal received by the 414 nm filter corresponds to the CH* emission while the other two filter show the diffuse background emission due to soot and broadband emission of the carbon dioxide. In image 9, the results for the air tests are show, it is clear that the signal in the 414 nm filter is strongest one. The background light emission will be present in all the wavelengths and act as a noise in the chemioluminescence signal. The image from the 469 nm filter provides an estimate of this noise in the CH* image. For the air coflow the signal in this wavelength was up to 3 times the estimate noise both with LPG(figure 9a) and Methane(figure 9b).

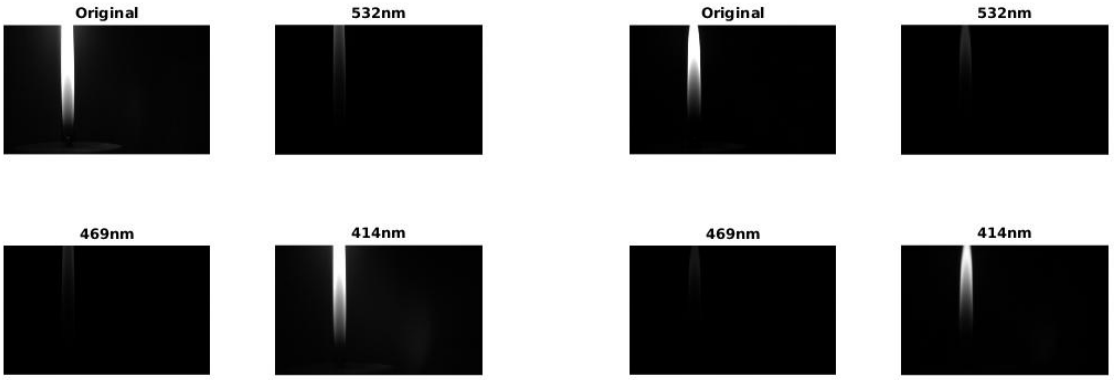

(a) LPG in Air (b) Methane in Air

Figure 9: Luminescence of flames in air

How the setup was kept constant an the only variation was the filter is possible to directly compare the images. Thus the filtered image signals were subtracted from the unfiltered image resulting in the picture 10. The subtraction show that most of the remain light was concentrated in the beginning of the flame, associate with other sources of emission specially the near ultra-violet emission of the OH* radical.

Figure 11 displays the results of the LPG oxy-fuel experiment. It is evident the change in format of the flame and reduction in brightness with the change in coflow composition. Observing all the images none of the oxy-fuel flames reach the size and brightness of the reference flame. The closest was the 30% oxygen with a similar size but with lower light emission.

Looking at the residual light(image 12)the contribution of the measured wavelengths also decreases resulting in greater remain light. Also the region of intense CH* emission shrinks and dislocate to the tip of the flame.

The same phenomena is present in the Methane flame but is more pronounce. Comparing image 13 with image 9b the combustion region was always significantly smaller and at 35% oxygen the flame was barely visible. In this scenario the residual light(figure 14) was greater than the LPG, also in the 40% oxygen experiment the difference between the residual and the original signal already is very subtle.

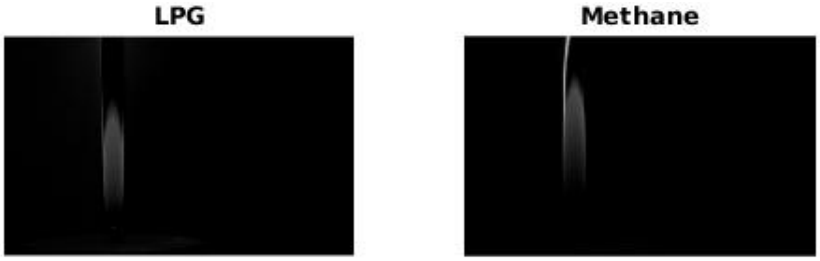

Figure 10: Residual Light

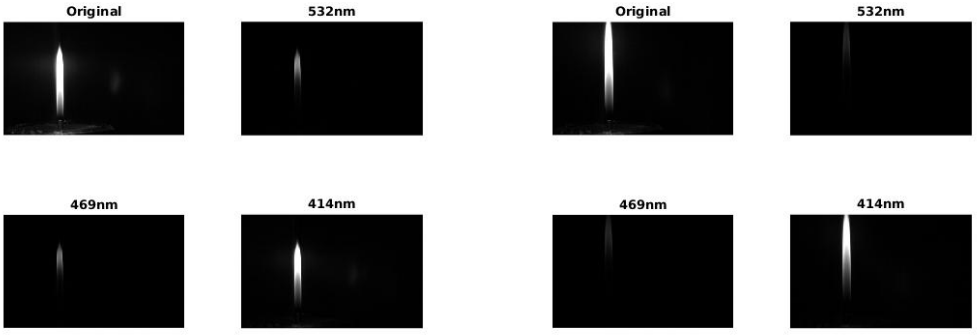

(a) 50% oxygen (b) 40% oxygen

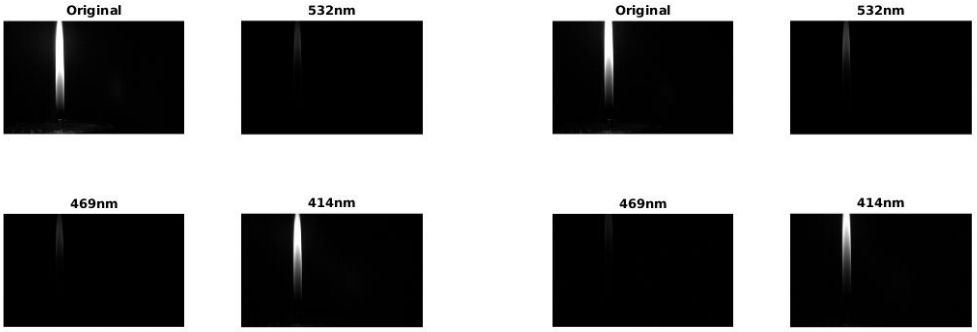

(c) 35% oxygen (d) 30% oxygen

Figure 11: Oxy-fuel LPG experiments

Due to the experimental procedures is also possible to sum the pixel value in the flame region to quantitative evaluate the amount of light emitted in total and in each wavelength approximating a spectrography. However, in some regions of the brighter images there were saturated pixels thus creating a bias in the data. This is a problem especially in the enriched oxy-fuel atmosphere(50% oxygen), but even in these cases is possible to draw some conclusion looking in to the integral value of the image. Picture 15 shows the proportional light emission of all the filters image and the residual light intensity. Experiments 1 and 2 are the air tests while 3 to 6 represents oxy-fuel LPG experiments with decreasing oxygen content(50%-40%-35%-30%) and 7 to 9 represents oxy-fuel methane experiments(50%-40%-35%). This graph can be used to evaluate the signal to noise relation in the CH* filter if the ratio of the 414 nm emission by the 469 nm emission is taken. Using this approach almost all experiments has a signal to noise relation greater than 3 with exception of the experiment number 9(methane in oxy-fuel enviroment 35% oxygen). In the oxy-fuel experiments the proportion of CH* light in the total emission reduces as the oxygen content drops, except from the 50% oxygen LPG case were there is an increase when compared with the next 40% oxygen atmosphere.

In figures 17 and 16, the relative amount of light in each case is studied comparing the reference case(air coflow) with the oxy-fuel for each fuel. The values of the sum of the pixels intensities is normalized by sum of the pixels in the reference image. The first observation is that all oxy-fuel flames presents a lower value than the reference. This happens because in this environment the flame is always smaller than the air flame. It size

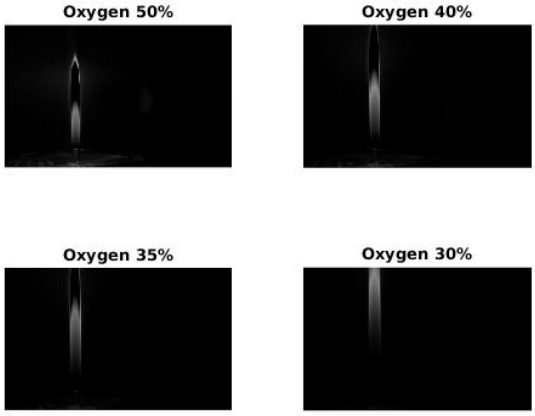

Figure 12: Residual Light for oxy-fuel LPG

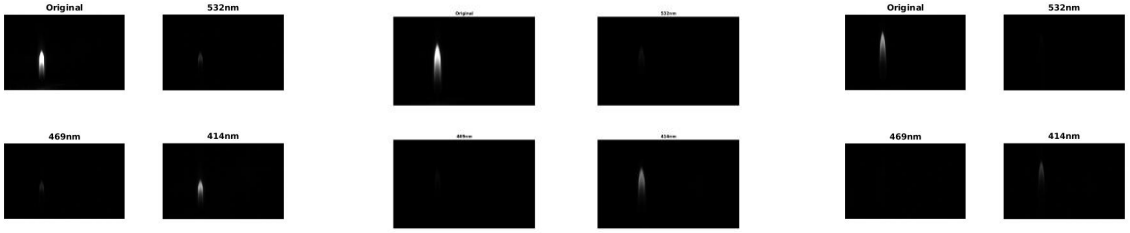

(a) 50% oxygen (b) 40% oxygen (c) 35% oxygen

Figure 13: Oxy-fuel Methane experiments

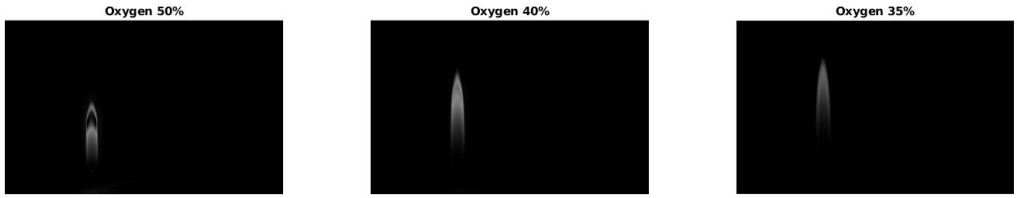

Figure 14: Residual Light for oxy-fuel Methane

tends to increase as the oxygen content drops, however this also reduces the light emission resulting in it never reaching the same luminosity as the air flame. Unfortunately, the saturation of the sensor in the 50% oxygen case LPG difficult a clear analysis and could explain the change in the behavior observed in the graphs. This effect is also clearly seen in the methane case specially in the CH* emission as it continually drops with the reduce in the oxygen.

To evaluate the shape and size of the reaction zone the Abel transform was applied to the total luminescence and CH* images. The object was to eliminate the superposition of the spacial emission zone in the image and estimate its real shape. The effect of such transform can be observed in the figure 18 in which the capture image is compared with its Abel transform. The transformed image presents an emission layer estimating the real size of the reaction zone. Moreover in the CH* emission a gray background and a salt and pepper noise is observed due to the lower signal to noise relation. To overcome this difficulty, the CH* oxy-fuel images were filtered by a Gaussian Blur and renormalized to display only the peak in light intensity and the its gradient. Figures 19a and 19b shows that as the amount of oxygen decreases the LPG flame becomes longer an the peak intensity in the CH* signal dislocate to the top of the flame an became weaker and more spread until in the least image is almost completely out of the measured region. This is also observed in the methane flame(images 20a and 20b) but is more pronounce. The CH* emission in the methane was more spread out and from the 40% test no clear peak was identified. This correlates with the results in the graph 15 and **??** were the CH* emission is smaller in all tested oxy-fuel, with higher residual and noise.

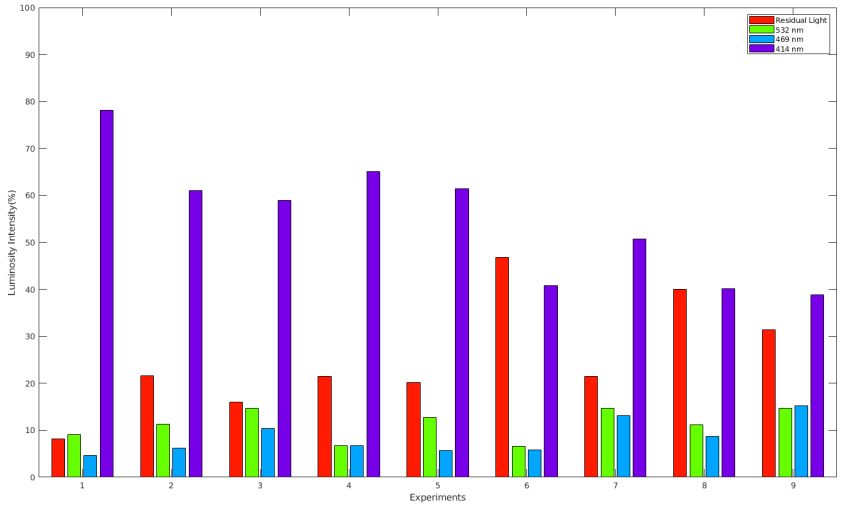

Figure 15: Total Light distribution, 1:LPG in air, 2:Methane in air, 3-6:LPG oxy-fuel,7-9 Methane oxy-fuel

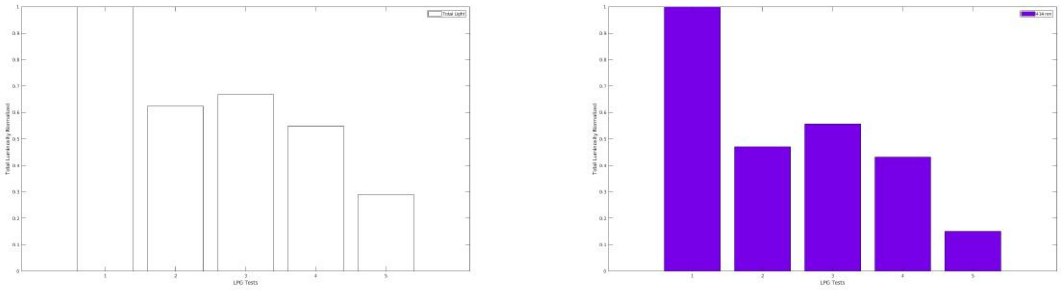

(a) Total luminosity (b) CH* filter

Figure 16: Relative pixel sum in the LPG tests

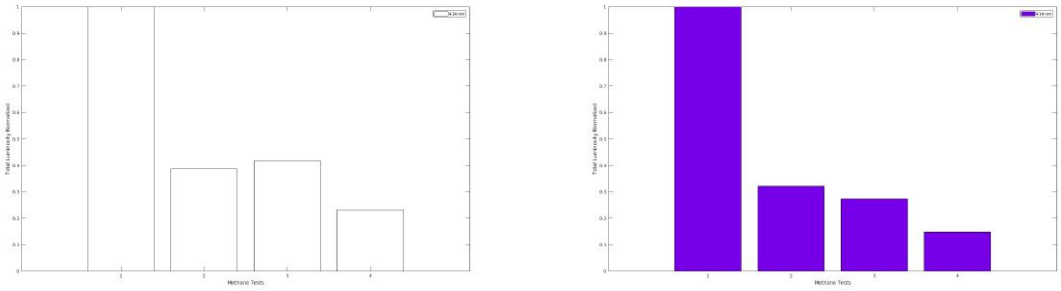

(a) Total luminosity (b) CH* filter

Figure 17: Relative pixel sum in the methane tests

7. CONCLUSION

The anemometer tests ensure the homogeneity of the coflow flow and characterize its turbulent proprieties. The problem with the initial non-homogeneity was solved by the reduction in the quantity of glass beads in the middle of the burner.

In the reactive flow tests, the first macroscopic result is the difference inferior oxygen limit between the methane and LPG. The LPG flame was kept stable until 30% oxygen and fade away right after the further reduction in the oxygen content. While the methane combustion could only be sustained in the 35% oxygen atmosphere, an explanation for this phenomena is that the methane molecule is more stable than the higher hydrocarbons of the LPG. Thus indicates a reduction in the oxidative potential even at 30% oxygen, an concentration almost 50% higher than the air. Further analyses in the acquired images(images 11 and 13) indicates

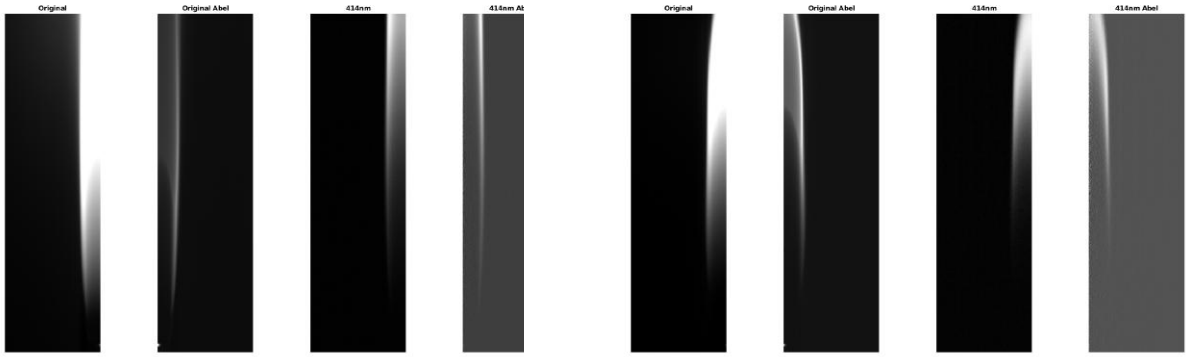

(a) LPG (b) Methane

Figure 18: Abel Transform of the signals

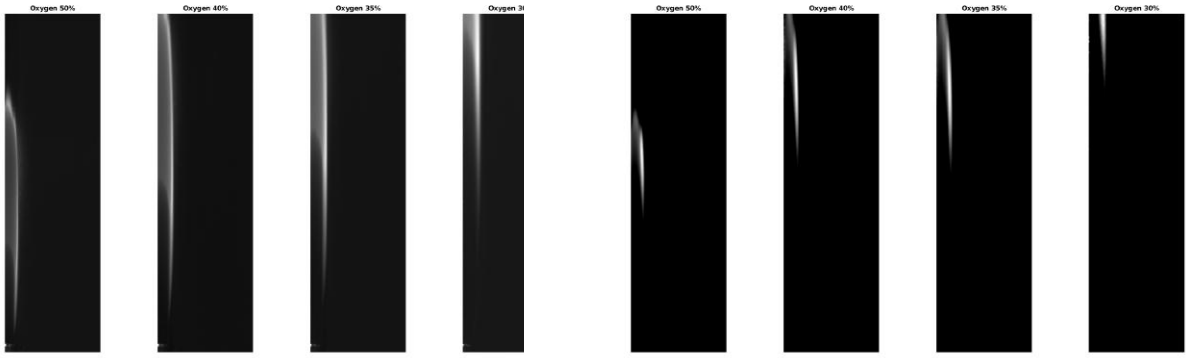

(a) Total light (b) CH* emission

Figure 19: Abel Transform of the Oxy-fuel LPG experiments

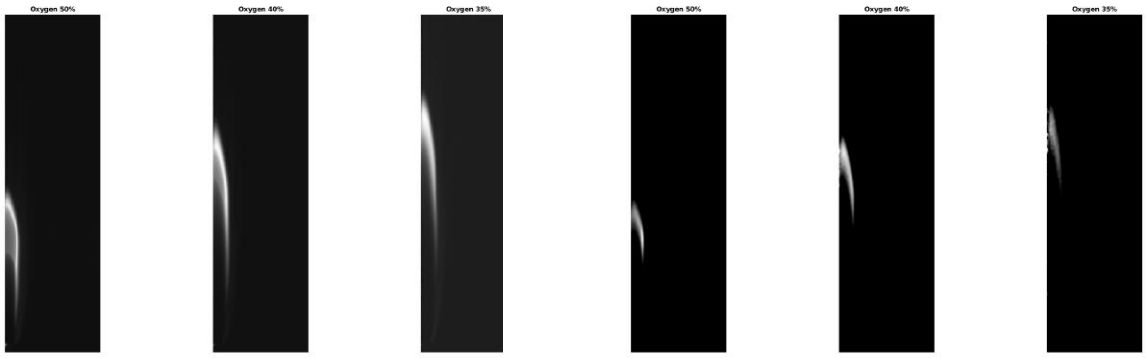

(a) Total light (b) CH* emission

Figure 20: Abel Transform of the Oxy-fuel Methane experiments

an smaller flame in all the cases when compared with the air case. That was an unexpected behavior because in principle the flame could achieve stability in the same position of the air with a specific oxygen concentration. However, not only the size but the measured luminosity was smaller. Also, the proportion of the CH* emission signal fall in relation to the total light received in all oxy-fuel tests being always smaller than it air counterpart(figure 15). Finally, the reaction zone evaluate through the Abel transform expand quickly with the reduction of oxygen. Only with the highest oxygen concentration the reaction zone was brighter and thinner than the air counterpart. The LPG also was less affected by the oxy-fuel environment than the methane, besides the flame enduring lower oxygen contents the images indicates a similar flame and CH* emission.

The causes to this change in the combustion are still open. This marked change even in a simple laminar flow indicates that oxy-fuel turbines may demand changes in the current designs to achieve efficient combustion. Combustion models also need to meet the generality of this scenario where some common hypothesis ,like unitary Lewis number, may not apply. This difference could be related to the greater specific heat of the carbon dioxide molecule, smaller diffusion coefficients, chemical interaction or all together. Further studies may approach with laminar premixed flames and high turbulence to evaluate the role of the change in diffusion. If diffusion is the major responsible for the behavior the effect should be less pronounce in high turbulence and more pronounce in laminar premixed flames. Another possibility is to use a noble gas, like argon, in replace of the carbon dioxide because this gas would not participate in the chemical reactions but has proprieties than nitrogen.

8. ACKNOWLEDGEMENTS

The authors would like to acknowledge Escola Politécnica da Universidade de São Paulo, Fundação de Ampáro à Pesquisa do Estado de São Paulo(FAPESP 2014/50279-4 and FAPESP 2013/5028-3) and Conselho Nacional de Desenvolvimento Científico e Tecnologico(CNPq) for the research support.

9. REFERENCES

Bennett, B.A.V., McEnally, C.S., Pfefferle, L.D., Smooke, M.D. and Colket, M.B., 2001. "Computational and experimental study of axisymmetric coflow partially premixed ethylene/air flames". *Combustion and Flame*, Vol. 127, No. 1-2, pp. 2004–2022.

Birol, F., 2017. "Key world energy statistics".

Chen, L., Yong, S.Z. and Ghoniem, A.F., 2012. "Oxy-fuel combustion of pulverized coal: Characterization, fundamentals, stabilization and cfd modeling". *Progress in energy and combustion science*, Vol. 38, No. 2, pp. 156–214.

De Leo, M., Saveliev, A., Kennedy, L.A. and Zelepouga, S.A., 2007. "Oh and ch luminescence in opposed flow methane oxy-flames". *Combustion and Flame*, Vol. 149, No. 4, pp. 435–447.

De Persis, S., Foucher, F., Pillier, L., Osorio, V. and Gökalp, I., 2013. "Effects of o2 enrichment and co2 dilution on laminar methane flames". *Energy*, Vol. 55, pp. 1055–1066.

Dworkin, S., Connelly, B., Schaffer, A., Bennett, B., Long, M., Smooke, M., Puccio, M., McAndrews, B. and Miller, J., 2007. "Computational and experimental study of a forced, time-dependent, methane–air coflow diffusion flame". *Proceedings of the Combustion Institute*, Vol. 31, No. 1, pp. 971–978.

Giménez-López, J., Millera, A., Bilbao, R. and Alzueta, M.U., 2015. "Experimental and kinetic modeling study of the oxy-fuel oxidation of natural gas, ch 4 and c 2 h 6". *Fuel*, Vol. 160, pp. 404–412.

Guiberti, T., Durox, D. and Schuller, T., 2017. "Flame chemiluminescence from co 2-and n 2-diluted laminar ch 4/air premixed flames". *Combustion and Flame*, Vol. 181, pp. 110–122.

Hardalupas, Y. and Orain, M., 2004. "Local measurements of the time-dependent heat release rate and equivalence ratio using chemiluminescent emission from a flame". *Combustion and Flame*, Vol. 139, No. 3, pp. 188–207.

Leung, D.Y., Caramanna, G. and Maroto-Valer, M.M., 2014. "An overview of current status of carbon dioxide capture and storage technologies". *Renewable and Sustainable Energy Reviews*, Vol. 39, pp. 426–443.

Panoutsos, C., Hardalupas, Y. and Taylor, A., 2009. "Numerical evaluation of equivalence ratio measurement using oh and ch chemiluminescence in premixed and non-premixed methane–air flames". *Combustion and Flame*, Vol. 156, No. 2, pp. 273–291.

Scheffknecht, G., Al-Makhadmeh, L., Schnell, U. and Maier, J., 2011. "Oxy-fuel coal combustion - a review of the current state-of-the-art". *International Journal of Greenhouse Gas Control*, Vol. 5, pp. S16–S35.

Smith, G.P., Luque, J., Park, C., Jeffries, J.B. and Crosley, D.R., 2002. "Low pressure flame determinations of rate constants for oh (a) and ch (a) chemiluminescence". *Combustion and Flame*, Vol. 131, No. 1-2, pp. 59–69.

Smooke, M., Long, M., Connelly, B., Colket, M. and Hall, R., 2005. "Soot formation in laminar diffusion flames". *Combustion and Flame*, Vol. 143, No. 4, pp. 613–628.

Smooke, M., McEnally, C., Pfefferle, L., Hall, R. and Colket, M., 1999. "Computational and experimental study of soot formation in a coflow, laminar diffusion flame". *Combustion and Flame*, Vol. 117, No. 1, pp. 117–139.

Sundkvist, S.G., Dahlquist, A., Janczewski, J., Sjödin, M., Bysveen, M., Ditaranto, M., Langørgen, Ø., Seljeskog, M. and Siljan, M., 2014. "Concept for a combustion system in oxyfuel gas turbine combined cycles". *Journal of Engineering for Gas Turbines and Power*, Vol. 136, No. 10, p. 101513.

Wall, T., Stanger, R. and Santos, S., 2011. "Demonstrations of coal-fired oxy-fuel technology for carbon capture and storage and issues with commercial deployment". *International journal of greenhouse gas control*, Vol. 5, pp. S5–S15.

Worth, N.A. and Dawson, J.R., 2012. "Tomographic reconstruction of oh chemiluminescence in two interacting turbulent flames". *Measurement Science and Technology*, Vol. 24, No. 2, p. 024013.

10. RESPONSIBILITY NOTICE

The authors are the only responsible for the printed material included in this paper.